Title:

Monophasic Action Potential Amplitude for Substrate Mapping

Brief Title:

Action Potential Mapping in Heart Failure

Manuscript Word Count: 3,044

Authors & Affiliations:

Ikeotunye Royal Chinyere [a,b], Mathew D Hutchinson [a,d], Talal Moukabary [a,c], Jordan J Lancaster [a], Steven Goldman [a,d], Elizabeth Juneman [a,d]

a. Sarver Heart Center, University of Arizona, Tucson, AZ
b. MD/PhD Program, College of Medicine, University of Arizona, Tucson, AZ
c. Carondelet Heart and Vascular Institute, Tucson, AZ
d. Division of Cardiology, Banner – University Medical Center, Tucson, AZ

* No conflicts of interest nor disclosures exist for all authors

Contributions:

IRC – main investigator, performed all data acquisition and analysis
MDH – clinical EP physician, provided equipment and guidance
TM – clinical EP physician, provided clinical context
JJL – research scientist, assisted with model creation
SG – co-principal investigator, provided scientific guidance
EJ – co-principal investigator, provided scientific guidance

Funding:

This work was supported by the NHLBI T32 HL007249-43, WARMER Research Foundation, Sarver Heart Center, University of Arizona, Hansjörg Wyss Foundation, and The Martin and Carol Reid Charitable Remainder Trust.

Corresponding Author:

Ike Chinyere

Sarver Heart Center

University of Arizona

1501 North Campbell Avenue, Room 6154

Tucson, AZ, 85724

P: (520)-626-2939

F: (520)-626-8080

ichinyere@email.arizona.edu

Acknowledgements:

A special thank you to Maribeth Stansifer, Sherry Daugherty, Mary Kaye Pierce, Mark Borgstrom, and Dr. Nancy K Sweitzer for their technical assistance.

Abstract:

Introduction

While radiofrequency ablation has revolutionized the management of tachyarrhythmias, the rate of arrhythmia recurrence is a large drawback. Successful substrate identification is paramount to abolishing arrhythmia and bipolar voltage electrogram's narrow field of view can be further reduced for increased sensitivity.

In this report, we perform cardiac mapping with monophasic action potential (MAP) amplitude. We hypothesize that MAP amplitude (MAPA) will provide more accurate infarct sizes than other mapping modalities via increased sensitivity to distinguish healthy myocardium from scar tissue.

Methods

Using the left-coronary artery ligation Sprague Dawley rat model of ischemic heart failure, we investigate the accuracy of *in vivo* ventricular epicardial maps derived from MAPA, MAP duration to 90% repolarization ($MAPD^{90}$), unipolar voltage amplitude (UVA), and bipolar voltage amplitude (BVA) when compared to gold-standard histopathological measurement of infarct size.

Results

Numerical analysis reveals discrimination of healthy myocardium versus scar tissue using $MAPD^{90}$ ($p=0.0158$) and UVA ($p<0.001$) ($n=21$). MAPA and BVA decreased between healthy and border tissue ($p=0.0218$, $p=0.0015$ respectively) and border and scar tissue ($p=0.0037$,

0.0094 respectively). Contrary to our hypothesis, BVA mapping performed most accurately regarding quantifying infarct size.

Conclusions

MAPA mapping may have high spatial resolution for myocardial tissue characterization but was quantitatively less accurate than other mapping methods at determining infarct size. BVA mapping's superior utility has been reinforced, supporting its use in translational research and clinical EP labs. MAPA may hold potential value for precisely distinguishing healthy myocardium, border zone, and scar tissue in diseases of disseminated fibrosis such as atrial fibrillation.

New and Noteworthy:

Monophasic action potential mapping in a clinically relevant model of heart failure with potential implications for atrial fibrillation management.

Keywords:

action potential, voltage, mapping, rat

Introduction:

Catheter-based radiofrequency ablation premiered in the late 1980s, resulting in new management options for complex arrhythmias such as atrioventricular nodal re-entrant tachycardia, atrial fibrillation, and ventricular tachycardia. While the value of radiofrequency ablation is evolving [4], shortcomings do exist. Of great importance is the arrhythmia recurrence rate, which repeatedly exposes patients to risks such as tamponade and permanent pacemaker placement during or after repeat ablation procedures.

Bipolar voltage electrograms are optimal in the context of ablation in that the field of view is sufficiently narrow to eliminate far-field noise and provide an accurate depiction of the local electric potential. However, in unique diseases such as atrial fibrillation that contain diffuse interstitial fibrosis [3], bipolar voltage electrograms may not be appropriate. Atrial fibrillation is a formidable disease due to the major quality of life challenges of thrombosis and stroke. These challenges are not always adequately mitigated with current radiofrequency ablation techniques. Reducing the recurrence rate for atrial fibrillation patients from 40% [9] to a more acceptable value will likely require techniques capable of highly sensitive identification of myocardial areas with electrical instability, which includes but is not limited to a decrease in tissue voltage.

We hypothesized that monophasic action potential (MAP) amplitude (MAPA) mapping would provide more accurate infarct sizes, compared to other mapping modalities, via increased sensitivity to distinguish healthy myocardium from scar tissue. Advantages of MAPA mapping include its inherent qualities relating to uniformly small field-of-view [2, 8], electrode-orientation insensitivity [12], and high-fidelity correlation to intracellular transmembrane action potentials. In this study, we utilize an *in vivo* animal model to demonstrate clinical feasibility.

Methods:

Ischemic Heart Failure Model

All rats in this study received humane care in compliance with Institutional Animal Care and Use Committee-approved protocols at the University of Arizona and in compliance with the National Institutes of Health's 'Guide for the Care and Use of Laboratory Animals'. The male Sprague Dawley rat (Envigo, Indianapolis, IN) permanent left coronary artery ligation model was used as previously described [10,16,19].

Rats are inducted with 3% isoflurane, anesthetized with a Ketamine, Xylazine, Acepromazine, Atropine, and saline cocktail, volume loaded intraperitoneally, undergo a medial sternotomy and receive a permanent proximal left coronary artery ligature. SHAM-operated surgical control rats receive the same procedure, excluding coronary ligation. Post-surgery, rats are maintained on standard light/dark cycles, rat chow, and water ad-libitum for six weeks while ischemic heart failure (HF) develops.

At six weeks, echocardiography is used to evaluate left ventricular (LV) function (ejection fraction, end-diastolic pressure, peak-developed-pressure, ±dP/dt, and time constant of relaxation, tau), and a terminal invasive hemodynamic and electrophysiology (EP) study is performed. During the terminal study, the rat is anesthetized, intubated, and mechanically ventilated on a rectal probe-gated heated platform with electrocardiogram monitoring [10,19]. A three-French solid-state micromanometer-tipped catheter is equilibrated and inserted into the carotid artery and advanced through the aortic valve to collect left ventricular hemodynamic parameters. Mapping is then performed using custom software system by collecting data from

roughly equidistant points in matrix format from the epicardial surface and interpolating the numerical data into color maps.

Monophasic Action Potential Acquisition

In vivo MAPs were obtained using a tungsten concentric bipolar microelectrode (instrument #TM53CCINS, World Precision Instruments, Sarasota, FL; Link). This superficially-penetrating microelectrode has a cone-shaped tip with a tip diameter of 3 micrometers, a tip electrode length of 250 micrometers, an electrode spacing of 300 micrometers, a ring electrode length of 200 micrometers and an impedance of 15KΩ. All EP signals were amplified with a BIOPAC MP150 data acquisition system and MCE100C amplifier modules (BIOPAC Systems, Inc., Goleta, CA; Link). Filtering settings for MAPs were as follows: 0.05 hertz high pass, 95 hertz low pass, and 60 hertz notch filter.

One-second intramural recordings (sedated rat heart rate is approximately 400 beats per minute) were obtained from twenty-four epicardial points within a matrix of six columns, each containing four rows; the matrix dimensions approximated 10 millimeters for each row in the y-axis and 15 millimeters for each column in the x-axis. Analysis included selecting three representative ventricular MAP that contained a stable baseline consistent with the two adjacent action potentials, and followed the general principles describing MAP phases [14]. Amplitude is defined as the millivoltage difference between phase four and the peak of phase zero. Ninety percent repolarization was selected for analysis, as oppose to a different percentage, to capture the well-described phenomenon of impaired late ventricular cardiomyocyte repolarization in ischemic heart failure [7, 13].

Voltage Electrogram Acquisition

One second voltage electrograms were obtained at the same ventricular epicardial MAP points with a clinical four-French quadripolar catheter (Bard Electrophysiology, Covington, GA). The four electrodes are one millimeter in length, each separated by one millimeter. Only two electrodes were utilized for data collection to ensure good contact with the ventricular epicardium. Analysis included filtering (0.05 hertz high pass, 240 hertz low pass, and 60 hertz notch filter) and selecting three representative tracing that contained a stable baseline consistent in the two adjacent tracings and followed the general principles in describing unipolar and bipolar electrogram waves. Amplitude is defined as peak-to-peak voltage, more specifically either Q-R, R-S, isoelectric line-R, or isoelectric line-QS.

Electrophysiological Mapping

While the primary area of interest is the ventricular scar and border region, the healthy ventricular myocardium is equally important, particularly the nonlinear interface of healthy and scar tissue. In this left coronary-ligation model, gross scar boundaries can be distinguished on the anterior left ventricular myocardium with the naked eye; this helped ensure that healthy myocardium, adjacent border tissue, and scar tissue were mapped. MAPA, MAP duration to 90% repolarization ($MAPD^{90}$), unipolar voltage electrogram amplitude (UVA), and bipolar voltage electrogram amplitude (BVA) values were assigned a color using a clinically-relevant color bar scheme.

The true distinction between normal and abnormal EP values for all mapping modalities was determined using a normal distribution cutoff, specifically the ±second standard deviation. The sign of second standard deviation depended on the parameter in analysis. For example, with

chronic ischemia, compromised cardiomyocyte action potential durations are expected to increase (+2S.D.) [7, 13], whereas compromised cardiomyocyte action potential amplitudes are expected to decrease (-2S.D.). Border values were calculated to be ten percent of the abnormal values adjacent to the normal-abnormal cutoff. All matrix values were then interpolated into a color map representing the epicardial surface spanning heathy myocardium to scar tissue.

Percentage of infarcted ventricular myocardium was extrapolated from color maps by comparing the two-dimensional surface area of scar tissue to the total area of the color map, which included healthy myocardium and border zone.

The same ventricular epicardial area was mapped in every rat, within a negligible error rate, because a single surgeon performed all median sternotomies, creating a surgical window of identical size in every rat. Furthermore, as mentioned before, the border of scar tissue is visible to the naked eye and was utilized to guide the placement of graded surgical marker boundaries.

Ex Vivo Histopathological Infarct Sizing

After hemodynamic and EP evaluation, all rats were sacrificed via three milliliter potassium chloride intracavitary injection. The heart was immediately excised from the mediastinum, flushed intracavitary with heparinized saline, formalin-fixed at 100 mmHg in a Langendorff preparation and stored for twenty-four hours in a glass jar. The fixed heart was then primed by removing non-left ventricular tissue and the remaining left ventricle was sent to an institutional core laboratory (Tissue Acquisition and Cellular/Molecular Analysis Shared Resource – University of Arizona Cancer Center) for staining and embedding. Left ventricle samples were sectioned by applying two equidistant cuts creating three portions (apex, mid, and base) and then stained with Masson's trichrome to distinguish between healthy myocardium and

scar tissue for histopathological circumferential infarct sizing [15]. Only the mid section was utilized for infarct sizing.

This circumference-based method was utilized, as opposed to an area-based method, to best approximate the two-dimensional surface area evaluated by the EP mapping modalities. An area-based method to size an infarct includes not only the epicardial scar tissue, but also intra-myocardial scar tissue and endocardial scar tissue for a three-dimensional volume value (example: arbitrary units^3). The circumference-based method utilized in this study employed an average of epicardial and endocardial scar length based on previously published techniques [15] to yield a two-dimensional surface area value (example: arbitrary units^2).

Statistical Analysis

Data are presented as group mean ± standard error of the mean (SEM). Statistical significance is defined as a $p<0.05$. Unpaired two-tailed student's t tests were used to compare the location means (healthy, border, scar) within the two groups (SHAM and HF) as well as between groups.

In assessing the accuracy between EP color map-derived infarct size and histopathological infarct size, average percent difference was utilized. Percent difference is defined as the absolute value of the difference between the experimental color map value and the histology value, divided by the average of the two numbers, all multiplied by one hundred. Related-Samples Friedman's Two-Way ANOVA was performed on the percent difference values to determine statistical significance in mapping accuracy.

Results:

Ischemic Heart Failure Model

Induction of HF in infarcted rats was confirmed by echocardiography and invasive hemodynamic measurements at six weeks post-MI (n=6 SHAM; n=11 HF). The LV ejection fraction decreased from 74±3 to 39±4% ($p<0.001$), LV peak-developed-pressure fell from 189±4 to 140±12 mmHg ($p=0.0104$), LV +dP/dt decreased from 7853±417 to 5360±393 mmHg/second ($p=0.0011$), and time constant of LV relaxation, tau, increased from 20±1 to 28±3 milliseconds ($p=0.0752$). LV end-diastolic pressure increased from 7±1 to 19±4 mmHg ($p=0.0470$) and LV -dP/dt increased from -6864±343 to -3981±490 mmHg/second ($p=0.0011$).

Monophasic Action Potential Acquisition

MAPs obtained (Figure 1) exhibited expected morphology for rat ventricular cardiomyocytes [14]. Approximately 7% of MAPs obtained from dense scar were unusable, the highest percentage from any tissue type. For SHAM rats (n=6), MAPA and $MAPD^{90}$ did not differ in any of the three zones, namely healthy (H), border (B), and scar (S) (Figure 2). However, in HF rats (n=21), MAPA decreased between H and B ($p=0.0015$), as well as between B and S ($p=0.0094$), while $MAPD^{90}$ only increased between the H and B ($p=0.0158$).

Voltage Electrogram Acquisition

Voltage tracings were of high resolution (Figure 3) and followed expected wave morphology for both unipolar and bipolar. Approximately 1% of MAPs obtained from dense scar were unusable, the highest percentage from any tissue type. For SHAM rats (n=6), UVA and BVA did not differ in any of the three zones (Figure 4). However, in HF rats (n=21), UVA and

BVA both decreased in the infarcted myocardium. UVA decreased between H and S ($p<0.001$), while BVA decreased between H and B ($p=0.0218$) as well as between B and S ($p=0.0037$).

Electrophysiologic Mapping

Of the total twenty-one HF rats, six representative rats were selected for color map infarct sizing comparison due to superior histopathology specimen quality (Figure 5, 6). Using Masson's trichrome histopathology stain as the gold-standard, BVA was found to be the most accurate method of approximating the size of the infarct region followed by UVA then MAPA (Figure 5). Statistical significance distinguished $MAPD^{90}$ from BVA ($p=0.010$). Qualitative assessment supported the notion of MAPA's superior spatial resolution (Figure 6, 7), despite MAPA not being the most accurate mapping method for determining infarct size.

Discussion:

This report defends the utility of MAPA as a mapping parameter and reinforces its robustness in *in vivo* cardiac EP applications. Although not as useful as BVA for quantifying scar tissue, these qualitative data (Figure 6, 7) may suggest that MAPA mapping attains a high degree of spatial resolution for distinguishing healthy, partially impaired, and grossly impaired cardiac tissue. We believe this may be due to the intrinsic qualities of MAPs relating to narrow field-of-view, electrode-orientation insensitivity, and ultra-sensitivity to aberrations. These findings may hold potential value for clinical procedures relating to high-fidelity mapping [18] (ex.: accessory pathway ablation [1], rotor termination [11]).

While MAPAs ultra-sensitivity to impaired depolarization asserts its utility in carefully dissecting substrate with respect to membrane potential, it also limits MAPAs clinical value with

respect to infarct sizing. The data suggest that MAPA attains high spatial resolution (Figure 6) yet MAPA fails to most accurately depict infarct size (Figure 5). This finding indicates that MAPA's sensitivity to 'electrical infarct' may render it relatively impervious to 'histopathologic infarct', as there is work supporting the notion that the two are not one-in-the-same [20].

Perhaps BVA provides the most accurate depiction of infarct size by averaging the optimal number of cardiomyocytes' electrical potentials to detect macro-irregularities, which have a stronger correlation to histopathologic infarct, rather than the micro-irregularities of MAPA. While detecting ultrastructural subtleties with MAPA may be important in specific clinical cases such as atrial fibrillation, overall, it seems to provide too sensitive of data and currently there are no approved clinical therapies that are evaluated via halting or reversing adverse remodeling at this microscopic tissue level.

In Figure 5, including the border zone surface area in the calculation of infarct size decreases the average percent difference of MAPA to levels comparable to BVA, suggesting that any deviation from normal phase zero-one activity has a stronger correlation to histopathologic scar. While utilizing the negative second deviation as a cutoff for MAPA seemed to underestimate the histopathologic infarct size, the same cutoff value was utilized for BVA which produced overestimates (Figure 5). We suspect that this is due to the previously mentioned qualities of MAPA and BVA relating to field-of-view: BVA averages the electrical potential from a larger population of cardiomyocytes and can overlook general anatomic variants in voltage such as endocardial trabeculations, while still achieving sufficient sensitivity to distinguish healthy myocardium from border zone and border zone from scar tissue (Figure 4).

Action potential duration is a common parameter used to measure cardiomyocyte damage from ischemia [6]. We have shown that MAPA has a greater ability than $MAPD^{90}$ to distinguish

the infarcted myocardium tissue types (Figure 2). The inferior ability of $MAPD^{90}$ to accurately quantify infarct size may relate to the excessive finesse of MAPs. These recordings are particularly susceptible to artifact given the small margin of repolarization voltages and the stepwise return to isoelectric potential that is easily affected by operator-mediated contact error or minor cell damage. Furthermore, improper electrode contact or epicardial collagen insulation may yield inappropriately small MAPs, which would affect the $MAPD^{90}$ to a greater extent than the MAPA by depicting nearly normal repolarization times even in the face of overt impaired repolarization. This theory may have been exhibited in this study, leading to $MAPD^{90}$ color maps depicting healthy myocardium where all other mapping modalities depict scar tissue (Figure 6, 7b).

UVA and BVA are both highly utilized in the clinical EP laboratory, particularly bipolar voltage electrograms for defining substrate. We included these parameters in our study (Figure 4) to assess the potential clinical application of creating myocardial maps with MAPA. Statistical analysis reveals that MAPA maps are inferior to both UVA and BVA maps when quantifying histopathologic infarct size (Figure 5), suggesting that quantifying scar tissue quantity and creating high-resolution epicardial maps are distinct tasks that warrant individualized techniques.

Limitations

In this body of work, we utilize *in vivo* cardiac EP parameters to estimate the location and amount of histopathologic scar. Due to the fact that perturbations in action potentials or electrograms do not unequivocally correspond with scar tissue, we acknowledge that an EP map-derived percentage scar value could be identical to a histopathologic percentage scar value, but be unrelated with respect to anatomic location. However, we contend that this phenomenon is not

confounding the results of this study, particularly because of the normal distribution cutoff criteria.

MAPs, particularly the third phase, have high sensitivity to electrode motion and contact pressure artifacts [5] and therefore are more likely to exhibit atypical morphology which may obscure the landmarks necessary for analysis. Nonetheless, MAPs have a high-fidelity correlation to intracellular transmembrane action potentials [17] and the methods for training the surgeon-electrode handler, acquiring the data with immediate review, and selecting representative tracings during post-acquisition processing in our study attempted to minimize artifacts by seeking consistent electrical activity. The fact that only 7% of MAPs from dense scar were unusable highlights our approach's reproducibility.

Scar tissue is a non-uniform three-dimensional structure that may not be fully encapsulated by a two-dimensional histopathology approximation (example: arbitrary units^2) such as the one employed in this study. Nonetheless, our work attempted to depict the epicardial layer of the healthy tissue-scar tissue interface in two dimensions and not the entire three-dimensional scar structure. We utilized a circumference-based histopathology infarct sizing methodology to simplify the scar to transmural thickness.

While this study is posed as LV mapping, a portion of the color maps involved the right ventricle-septum border, which served as healthy myocardium. This was done in order to create a uniform area of mapping in all rats, as some infarcted rats have extensive anterior LV scar consequent to efficacious coronary ligation. We did not object to involving a portion of the right ventricle-septal border because the thickness difference between the right ventricle (RV) and LV in rats is less pronounced compared to humans' RV-LV thickness difference, mainly for two

reasons: 1) substantially smaller body habitus 2) quadrupedal stature, lessening the antagonism of gravity on systemic circulation.

Finally, a different method to define infarct size is cardiac magnetic resonance imaging. We acknowledge that cardiac magnetic resonance imaging-based computations would have served as a more clinically relevant gold-standard method to quantify the infarct size *in vivo*, as opposed to the histopathology we utilized in this work.

Conclusion:

We describe the creation of electrophysiologic color maps using the ventricular epicardial parameters of MAPA, $MAPD^{90}$, UVA, and BVA. To our knowledge, this is the first attempt to utilize MAPA for two-dimensional mapping in an *in vivo* animal model and is also the first to compare four different mapping modalities simultaneously to assess infarct sizing and spatial resolution.

We hypothesized that MAPA mapping would provide more accurate infarct sizes via increased sensitivity to distinguish between healthy myocardium and scar tissue, compared to the other mapping modalities. Using a rat model of ischemic heart failure, we quantified the percentage of infarcted myocardium from each two-dimensional map and determined that BVA maps create the most accurate depiction of percentage of infarcted myocardium, relative to histopathology. While MAPA is not of the same power with respect to depicting infarct size, it may be useful for characterizing convoluted ischemic myocardial pathways in atrial fibrillation.

Figure 1: Monophasic Action Potential Tracings

Fig 1: All MAP tracings are from a single HF rat's ventricular epicardium. The x-axis is time in seconds; the y-axis is amplitude in millivolts. The highest amplitude (gray) tracing represents healthy myocardium (H). The intermediate-amplitude (yellow, dashed) tracing represents tissue border (B) to scar tissue (S), depicted in red.

Figure 2: Monophasic Action Potential Data

Fig 2: a) An *ex vivo* HF heart with an example EP color map of four rows and six columns. Each black dot represents a mapped point, and each dot's label hypothetical. b) MAP data for SHAM (n=6) and HF (n=21). The MAP parameters are amplitude, in millivolts, and duration at ninety percent repolarization, in milliseconds. Values are reported as mean +SEM. * denotes significance (t test, $p<0.05$) versus Scar, # denotes significance (t test, $p<0.05$) versus Border.

Figure 3: Unipolar and Bipolar Voltage Electrogram Tracings

Fig 3: All unipolar (a) and bipolar (b) voltage electrogram tracings are from a single HF rat's ventricular epicardium. The x-axis is time in seconds; the y-axis is amplitude in millivolts. The highest amplitude (grey) tracing represents healthy tissue (H). The intermediate-amplitude (yellow, dashed) tracing represents tissue border (B) to scar (S), depicted in red.

Figure 4: Voltage Electrogram Data

Fig 4: See Figure 2a for reference. Unipolar and bipolar voltage electrogram data for SHAM (n=6) and HF (n=21). The electrogram parameter is voltage amplitude, in millivolts. Values are reported as mean +SEM. * denotes significance (t test, $p<0.05$) versus Scar, # denotes significance (t test, $p<0.05$) versus Border.

Figure 5: Mapping versus Histopathology Infarct Sizing

Fig 5: Comparison of six rats' infarct size derived from different methods of EP mapping, namely monophasic action potential (MAP) amplitude (MAPA), MAP duration to ninety percent repolarization ($MAPD^{90}$), unipolar voltage electrogram amplitude (UVA), and bipolar voltage electrogram amplitude (BVA). 'au' for arbitrary units. BVA is the most consistently accurate in approximating histopathological infarct size. * denotes significance versus BVA (Related-Samples Friedman's Two-Way ANOVA, p=0.010).

Figure 6: Color Maps and Histopathology Sections

Fig 6: Images for the same six rats highlighted in Figure 5. Color maps generated from the four different methods of EP mapping, namely MAPA, $MAPD^{90}$, UVA, and BVA, with a single corresponding histopathological section (mid). At the top of each column, the color bar for each mapping modality can be found, with black bars approximating the value threshold between each tissue type. For orientation, asterisks on histopathology slices denote where the right ventricle was removed. The dotted lines on the histopathology sections approximate the mapped epicardium and portion of histopathology included in infarct sizing (black star). While most maps contain scar tissue on the right side, $MAPD^{90}$ maps have obvious flaws, suggesting an incapability to determine infarcted tissue *in vivo*.

Figure 7: Mapping Percent Scar versus Histopathology Percent Scar

Fig 7: MAPA (panel a), MAPD90 (panel b), UVA (panel c), and BVA (panel d) maps are depicted for a single HF rat. Histopathology slides relative to the specific mapped epicardium of the same HF rat (panel e). For orientation, asterisks on histopathology sections denote where the right ventricle was removed. The circles (panels a, e) suggest MAPA's high spatial resolution, distinguishing adjacent healthy and scar tissue (4X magnification). The red circle highlights epicardial collagen insulation; the black dotted circle highlights diffuse scar infiltration; the double yellow circle highlights normal myocardium.

References:

[1] **Badger TJ, Daccarett M, Akoum NW, Adjei-Poku YA, Burgon NS, Haslam TS, Kalvaitis S, Kuppahally S, Vergara G, McMullen L, Anderson PA, Kholmovski E, MacLeod RS, Marrouche NF**. Evaluation of Left Atrial Lesions after Initial and Repeat Atrial Fibrillation Ablation: Lessons Learned from Delayed-Enhancement MRI in Repeat Ablation Procedures. *Circulation: Arrhythmia and Electrophysiology* 3(3): 249-259, 2010.

[2] **Brunckhorst CB, Delacretax E, Soejima K, Maisel WH, Friedman PL, Stevenson WG**. Impact of Changing Activation Sequence on Bipolar Electrogram Amplitude for Voltage Mapping of Left Ventricular Infarcts Causing Ventricular Tachycardia. *Journal of Interventional Cardiac Electrophysiology* 12: 137-141, 2005.

[3] **Burstein B, Nattel S**. Atrial Fibrosis: Mechanisms and Clinical Relevance in Atrial Fibrillation. *Journal of the American College of Cardiology* 51(8): 802-809, 2008.

[4] **Cui J, Gonzalez MD, Blaha C, Hill A, Sinoway LI**. Sympathetic Responses Induced by Radiofrequency Catheter Ablation of Atrial Fibrillation. *American Journal of Physiology: Heart and Circulatory Physiology* 316: H476-H484, 2018.

[5] **Franz MR**. Method and Theory of Monophasic Action Potential Recording. *Progress in Cardiovascular Diseases* 33(6): 347-368, 1991.

[6] **Franz MR, Flaherty FT, Platia EV, Bulkley BH, Weisfeldt ML**. Localization of Regional Myocardial Ischemia by Recording of Monophasic Action Potentials. *Circulation* 69(3): 593-604, 1984.

[7] **Frommeyer G, Milberg P, Witte P, Stypmann J, Koopmann M, Lücke M, Osada N, Breithardt G, Fehr M, Eckardt L**. A New Mechanism Preventing Proarrhythmia in Chronic Heart Failure: Rapid Phase-III Repolarization Explains the Low Proarrhythmic Potential of Amiodarone in Contrast to Sotalol in a Model of Pacing-Induced Heart Failure. *European Journal of Heart Failure* 13: 1060-1069, 2011.

[8] **Hutchinson MD, Gerstenfeld EP, Desjardins B, Bala R, Riley MP, Garcia FC, Dixit S, Lin D, Tzou WS, Cooper JM, Verdino RJ, Callans DJ, Marchlinski FE**. Endocardial Unipolar Voltage Mapping to Detect Epicardial Ventricular Tachycardia Substrate in Patients with Nonischemic Left Ventricular Cardiomyopathy. *Circulation: Arrhythmia and Electrophysiology* 4: 49-55, 2011.

[9] **Joseph JP, Rajappan K**. Radiofrequency Ablation of Cardiac Arrhythmias: Past, Present, and Future. *QJM: An International Journal of Medicine* 105(4): 303-314, 2012.

[10] **Lancaster JJ, Juneman E, Arnce SA, Johnson NM, Qin Y, Witte R, Thai H, Kellar RS, Ek Vitorin J, Burt J, Gaballa MA, Bahl JJ, Goldman S**. An Electrically Coupled Tissue-Engineered Cardiomyocyte Scaffold Improves Cardiac Function in Rats with Chronic Heart Failure. *Journal of Heart and Lung Transplantation* 33(4): 438-445, 2014.

[11] **Luther V, Sikkel M, Bennett N, Guerrero F, Leong K, Qureshi N, Ng FS, Hayat SA, Sohaib SM, Malcolme-Lewis L, Lim E, Wright I, Koa-Wing M, Lefroy DC, Linton NW, Whinnett Z, Kanagaratnam P, Davies DW, Peters NS, Lim PB**. Visualizing Localized Reentry with Ultra-High Density Mapping in Iatrogenic Atrial Tachycardia. *Circulation: Arrhythmia and Electrophysiology* 10: e004724, 2017.

[12] **Magtibay K, Massé S, Asta J, Kusha M, Lai PFH, Azam MA, Porta-Sanchez A, Haldar S, Malebranche D, Labos C, Deno DC, Nanthakumar K**. Physiological Assessment of Ventricular Myocardial Voltage Using Omnipolar Electrograms. *Journal of the American Heart Association* 6(8): e006447, 2017.

[13] **Näbauer M, Kääb S**. Potassium Channel Down-Regulation in Heart Failure. *Cardiovascular Research* 37(1998): 324-334, 1998.

[14] **Nerborrne J, Kass RS**. Molecular Physiology of Cardiac Repolarization. *Physiological Reviews* 85(4): 1205-1253, 2005.

[15] **Takagawa J, Zhang Y, Wong ML, Sievers RE, Kapasi NK, Wang Y, Yeghiazarians Y, Lee RJ, Grossman W, Springer ML**. Myocardial Infarct Size Measurement in the Mouse Chronic Infarction Model: Comparison of Area- and Length-Based Approaches. *Journal of Applied Physiology* 102(6): 2104-2111, 2007.

[16] **Thai HM, Do BQ, Tran TD, Gaballa MA, Goldman S**. Aldosterone Antagonism Improves Endothelial-Dependent Vasorelaxation in Heart Failure via Upregulation of Endothelial Nitric Oxide Synthase Production. *Journal of Cardiac Failure* 12(3): 240-245, 2006.

[17] **Tse G, Wong ST, Tse V, Yeo JM**. Monophasic Action Potential Recordings: Which is the Recording Electrode? *Journal of Basic Clinical Physiology and Pharmacology* 27(5): 457-462, 2016.

[18] **Tung R**. Challenges and Pitfalls of Entrainment Mapping of Ventricular Tachycardia. *Circulation: Arrhythmia and Electrophysiology* 10: e004560, 2017.

[19] **Weigand K, Witte R, Moukabary T, Chinyere IR, Lancaster J, Pierce MK, Goldman S, Juneman E**. In vivo Electrophysiological Study of Induced Ventricular Tachycardia in Intact Rat Model of Chronic Ischemic Heart Failure. *Institute of Electrical and Electronics Engineers – Transactions on Biomedical Engineering* 64(6): 1393-1399, 2017.

[20] **Zheng Y, Fernandes MR, Silva GV, Cardoso CO, Canales J, Gahramenpour A, Baimbridge F, Cabreira-Hansen MDG, Perin EC**. Histopathological Validation of Electromechanical Mapping in Assessing Myocardial Viability in a Porcine Model of Chronic Ischemia. *Experimental and Clinical Cardiology* 13(4): 198-203, 2008.

Figure 1: Monophasic Action Potential Tracings

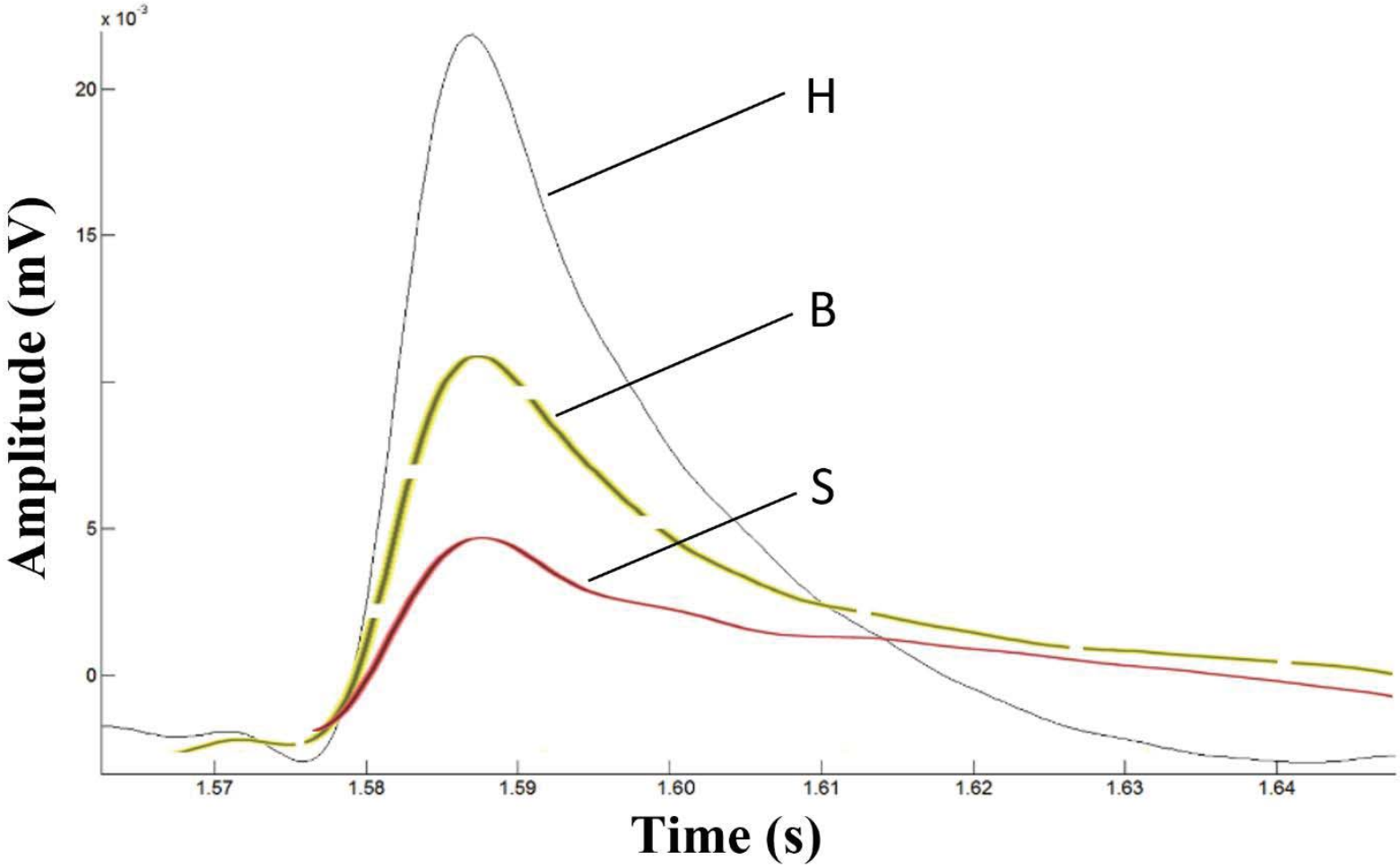

Fig 1: All MAP tracings are from a single HF rat's ventricular epicardium. The x-axis is time in seconds; the y-axis is amplitude in millivolts. The highest amplitude (gray) tracing represents healthy myocardium (H). The intermediate-amplitude (yellow, dashed) tracing represents tissue border (B) to scar tissue (S), depicted in red.

Figure 2: Monophasic Action Potential Data

a)

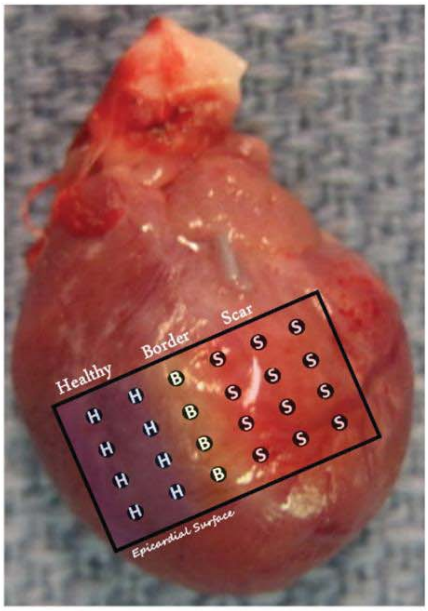

b)

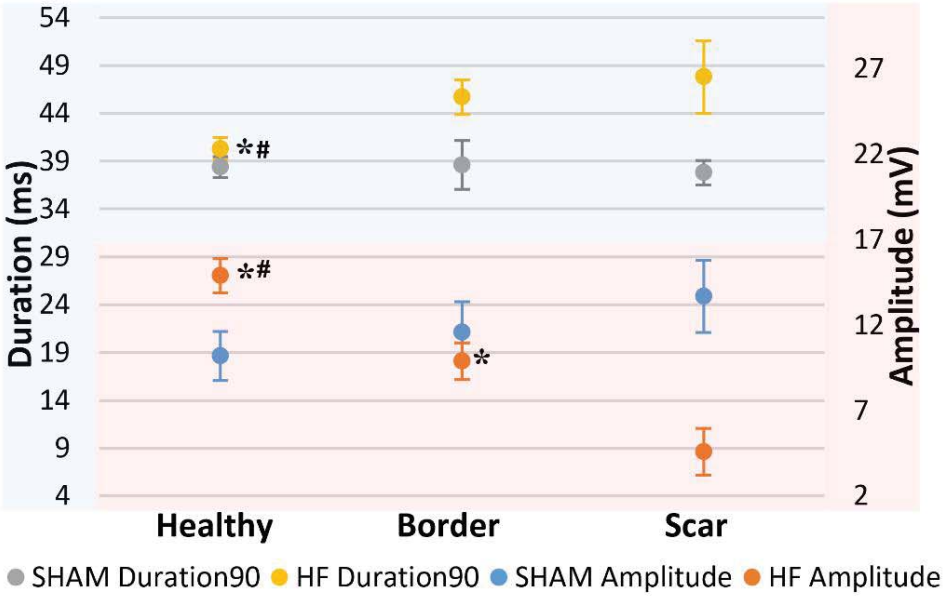

Fig 2: a) An *ex vivo* HF heart with an example EP color map of four rows and six columns. Each black dot represents a mapped point, and each dot's label hypothetical. b) MAP data for SHAM (n=6) and HF (n=21). The MAP parameters are amplitude, in millivolts, and duration at ninety percent repolarization, in milliseconds. Values are reported as mean +SEM. * denotes significance (t test, $p<0.05$) versus Scar, # denotes significance (t test, $p<0.05$) versus Border.

Figure 3: Unipolar and Bipolar Voltage Electrogram Tracings

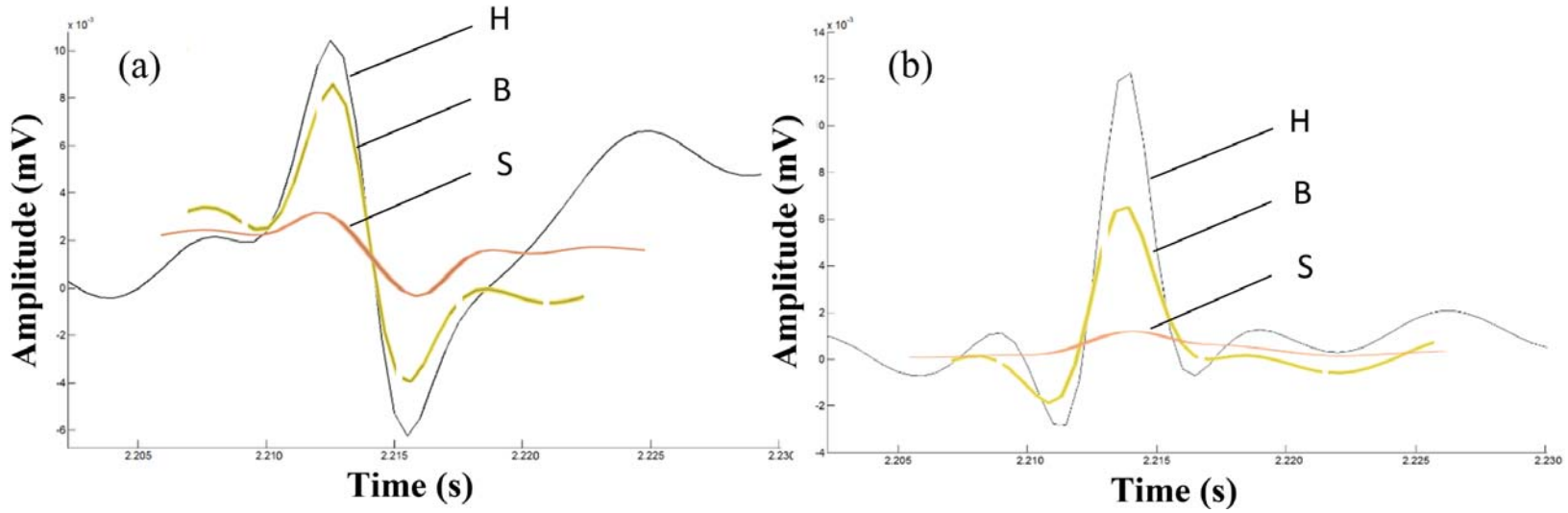

Fig 3: All unipolar (a) and bipolar (b) voltage electrogram tracings are from a single HF rat's ventricular epicardium. The x-axis is time in seconds; the y-axis is amplitude in millivolts. The highest amplitude (grey) tracing represents healthy tissue (H). The intermediate-amplitude (yellow, dashed) tracing represents tissue border (B) to scar (S), depicted in red.

Figure 4: Voltage Electrogram Data

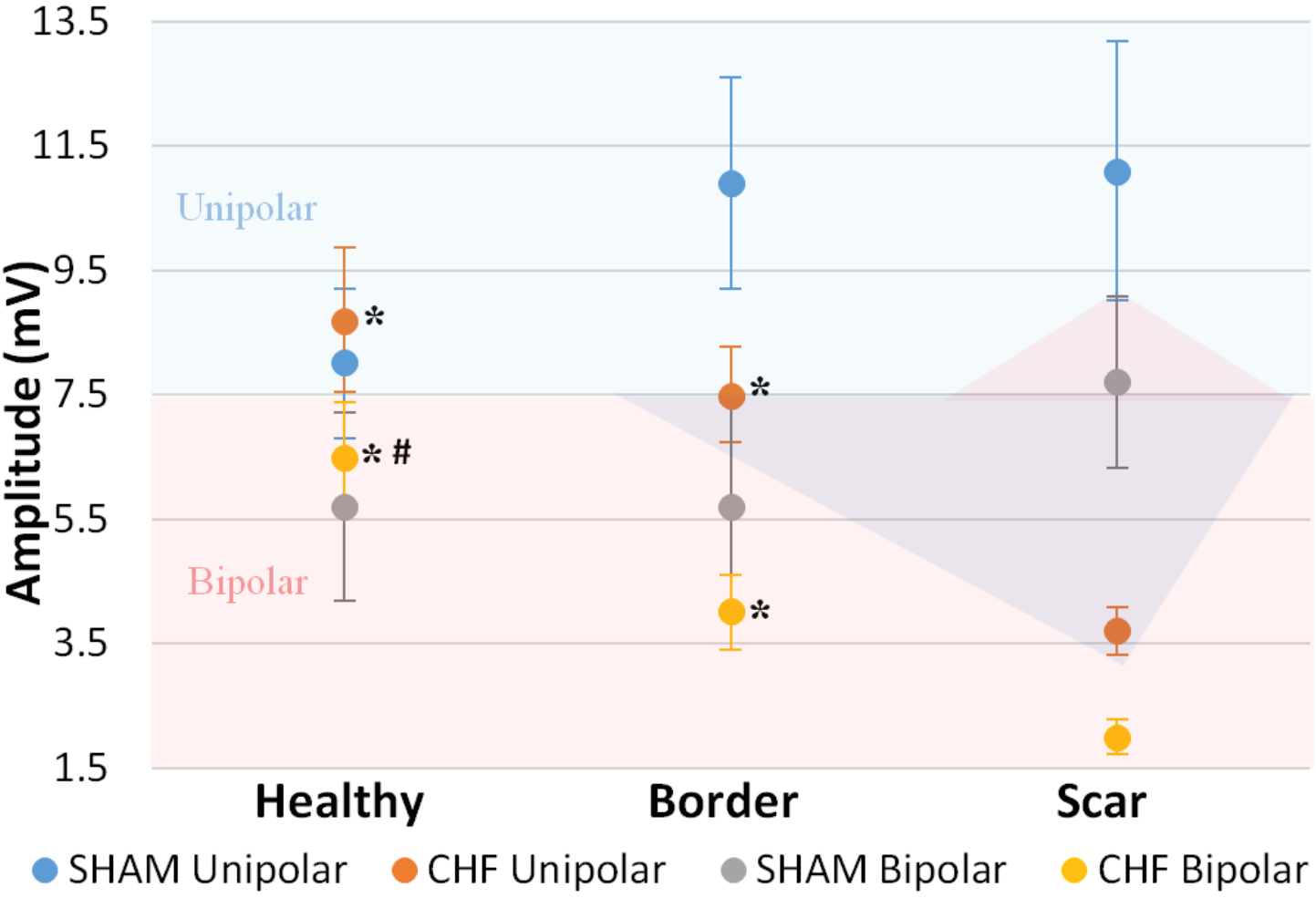

Fig 4: See Figure 2a for reference. Unipolar and bipolar voltage electrogram data for SHAM (n=6) and HF (n=21). The electrogram parameter is voltage amplitude, in millivolts. Values are reported as mean +SEM. * denotes significance (t test, $p<0.05$) versus Scar, # denotes significance (t test, $p<0.05$) versus Border.

Figure 5: Mapping versus Histopathology Infarct Sizing

Rat #	MAPA	$MAPD^{90}$	UVA	BVA	*Histopathology*
1	**0.29** au^2	**0.06** au^2	**0.61** au^2	**0.62** au^2	***0.54*** au^2
2	**0.39** au^2	**0.05** au^2	**0.49** au^2	**0.47** au^2	***0.28*** au^2
3	**0.32** au^2	**0.30** au^2	**0.49** au^2	**0.50** au^2	***0.47*** au^2
4	**0.27** au^2	**0.12** au^2	**0.65** au^2	**0.63** au^2	***0.50*** au^2
5	**0.31** au^2	**0.19** au^2	**0.52** au^2	**0.46** au^2	***0.38*** au^2
6	**0.42** au^2	**0.03** au^2	**0.56** au^2	**0.55** au^2	***0.39*** au^2
Average % Difference	36%	117%*	27%	24%	*0%*

Fig 5: Comparison of six rats' infarct size derived from different methods of EP mapping, namely monophasic action potential (MAP) amplitude (MAPA), MAP duration to ninety percent repolarization ($MAPD^{90}$), unipolar voltage electrogram amplitude (UVA), and bipolar voltage electrogram amplitude (BVA). 'au' for arbitrary units. BVA is the most consistently accurate in approximating histopathological infarct size. * denotes significance versus BVA (Related-Samples Friedman's Two-Way ANOVA, p=0.010).

Figure 6: Color Maps and Histopathology Sections

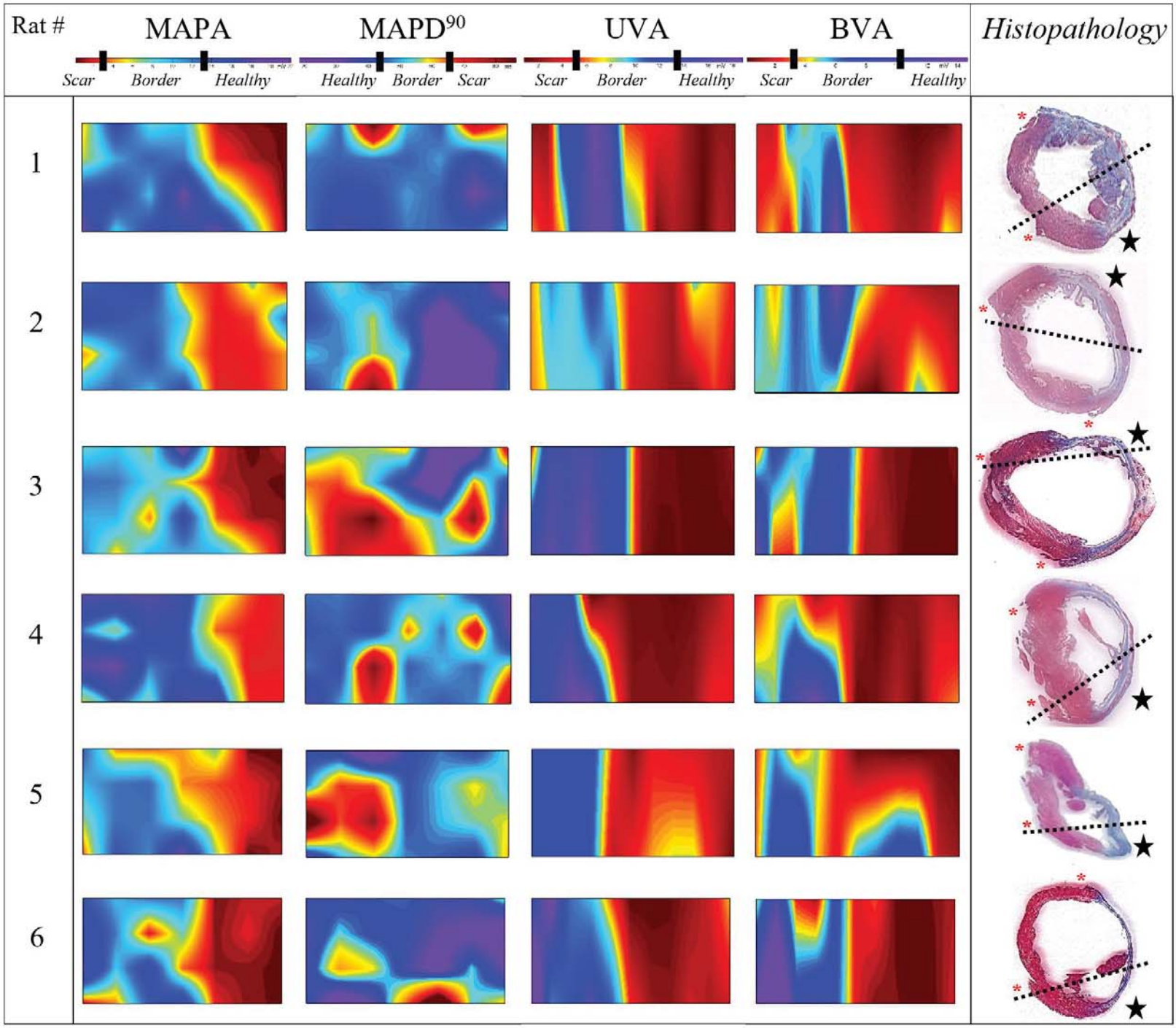

Fig 6: Images for the same six rats highlighted in Figure 5. Color maps generated from the four different methods of EP mapping, namely MAPA, $MAPD^{90}$, UVA, and BVA, with a single corresponding histopathological section (mid). At the top of each column, the color bar for each mapping modality can be found, with black bars approximating the value threshold between each tissue type. For orientation, asterisks on histopathology slices denote where the right ventricle was removed. The dotted lines on the histopathology sections approximate the mapped epicardium and portion of histopathology included in infarct sizing (black star). While most maps contain scar tissue on the right side, $MAPD^{90}$ maps have obvious flaws, suggesting an incapability to determine infarcted tissue *in vivo*.

Figure 7: Mapping Percent Scar versus Histopathology Percent Scar

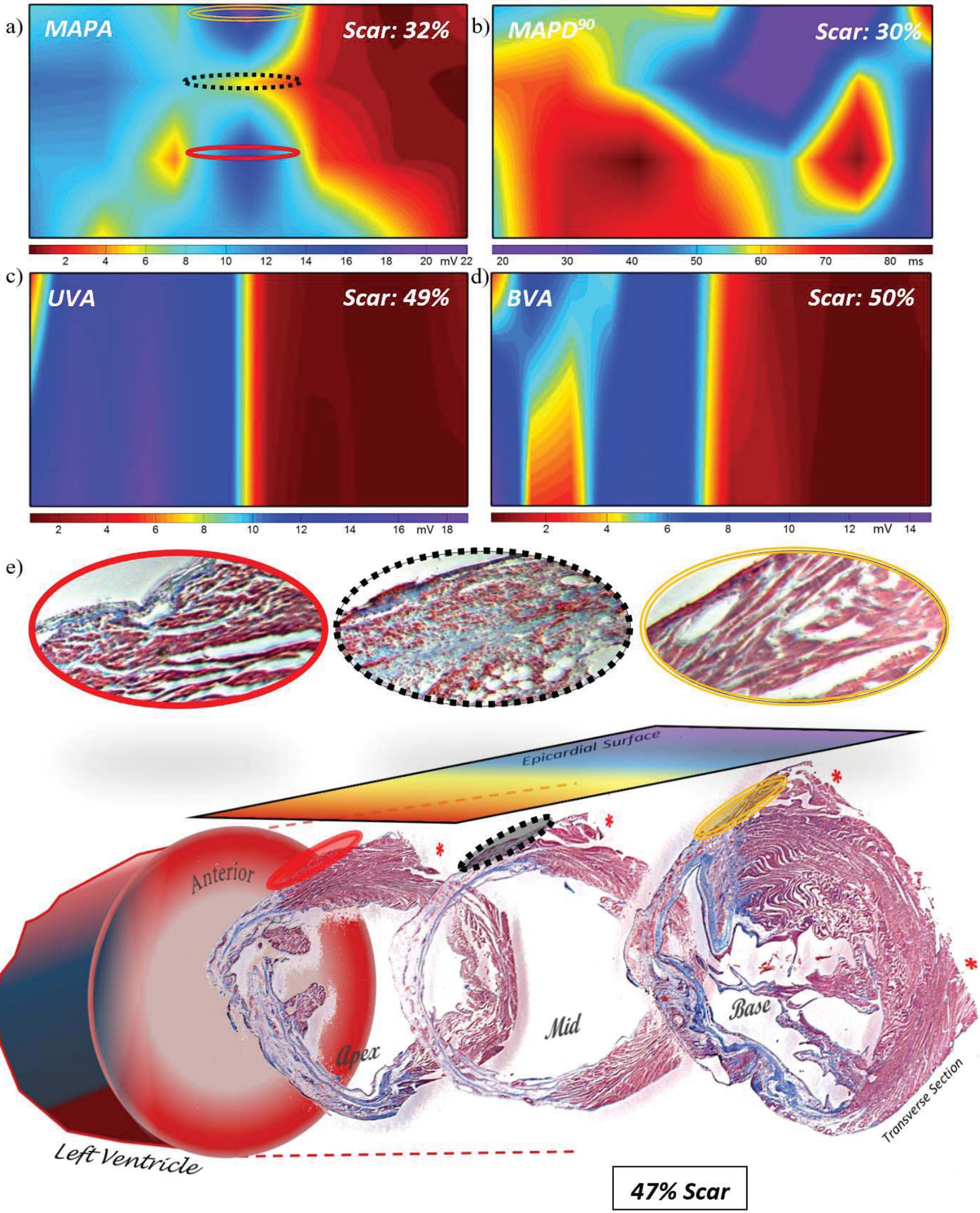

Fig 7: MAPA (panel a), MAPD90 (panel b), UVA (panel c), and BVA (panel d) maps are depicted for a single HF rat. Histopathology slides relative to the specific mapped epicardium of the same HF rat (panel e). For orientation, asterisks on histopathology sections denote where the right ventricle was removed. The circles (panels a, e) suggest MAPA's high spatial resolution, distinguishing adjacent healthy and scar tissue (4X magnification). The red circle highlights epicardial collagen insulation; the black dotted circle highlights diffuse scar infiltration; the double yellow circle highlights normal myocardium.